Fusion-fission dynamics of ^{188,190}Pt through fission fragment mass distribution measurements

Kavita,[1] K. S. Golda,[2] T. K. Ghosh,[3,10] A. Jhingan,[2] P. Sugathan,[2] A. Chatterjee,[2,9] B. R. Behera,[4] Ashok Kumar,[4] Rakesh Kumar,[1] N. Saneesh,[2] M. Kumar,[2] Abhishek Yadav,[2] C. Yadav,[2] Neeraj Kumar,[5] Akashrup Banerjee,[5] A. Rani,[5] S. K Duggi,[6] Rakesh Dubey,[7] Kavita Rani,[4] Shoaib Noor,[8] Jaimin Acharya,[9] and Hardev Singh[1,*]

[1]*Department of Physics, Kurukshetra University, Kurukshetra 136119, India*
[2]*Inter-university Accelerator Centre, Aruna Asaf Ali Marg, New Delhi 110067, India*
[3]*Variable Energy Cyclotron Centre, 1/AF, Bidhan Nagar, Kolkata 700064, India*
[4]*Department of Physics, Panjab University, Chandigarh 160014, India*
[5]*Department of Physics and Astrophysics, University of Delhi, Delhi 110007, India*
[6]*Department of Nuclear Physics, Andhra University, Visakhapatnam 530003, India*
[7]*iThemba LABS, National Research Foundation, Somerset West, South Africa*
[8]*Department of Physics, Thapar University, Patiala, Punjab 147004, India*
[9]*Department of Physic, M. S. University of Baroda, Vadodara, Gujarat 390002, India*
[10]*Homi Bhabha National Institute, Training School Complex, Anushakti Nagar, Mumbai 400094, India*

(Received 21 May 2019; published 27 August 2019)

Fission fragment mass distributions have been measured for relatively neutron-deficient compound nuclei, ^{188}Pt and ^{190}Pt, formed in the fusion reactions, ^{28}Si + ^{160}Gd and ^{12}C + ^{178}Hf, respectively. The data were obtained for a similar initial excitation energy range of 49–68 MeV for both the systems. The fragment mass distributions for both the Pt isotopes were found to be single peaked and no appreciable change in the mass symmetry was observed throughout the measured excitation energy range, for both the reactions. However, relatively broader mass distributions observed in the fission of ^{188}Pt in the studied energy domain indicates the presence of fission events originating from a nonequilibrated source as well. This signifies that the mass equilibrium has not been fully achieved in the ^{28}Si + ^{160}Gd system as compared to the ^{12}C + ^{178}Hf system, indicating the presence of quasifission events in the former reaction.

DOI: 10.1103/PhysRevC.100.024626

I. INTRODUCTION

One of the interesting topics of research in contemporary nuclear physics is the formation of superheavy elements (SHEs) by using the right choice of projectile and target combinations [1–6]. The ultralow formation cross sections combined with experimental difficulties in the production of SHEs makes such studies challenging. The formation phase interactions between the reaction observables plays a very important role in deciding the fate of the composite system. The relatively early reseparation of the composite system into the projectile-like and target-like fragments, which leads to the quasifission (QF) process, is one of the main hurdles in the synthesis of SHEs [7–10].

The product of charges (Z_PZ_T, where Z_P and Z_T are the atomic charges of the projectile and target, respectively) appears to play a key role in deciding the onset of QF [11–14] in heavy-ion-induced fusion-fission reactions. Theoretical models predicted the existence of QF in the reactions having $Z_PZ_T \geqslant 1600$ [12,15,16]. However, recent measurements have shown that nonequilibrium-like fission can exist for the fusion of lighter systems having $Z_PZ_T < 800$ [17–20]. Some of the other factors influencing the onset or presence of QF in such reactions are the direction of mass flow in the dinuclear system, which is governed by the relative value of entrance channel mass asymmetry [$\alpha = (A_T - A_P)/(A_T + A_P)$] with regard to the critical Businaro-Gallone mass asymmetry α_{BG} [21], deformation of the projectile and/or target nuclei [22–24], excitation energy of the compound system, fissility of the compound nucleus [25], N/Z of the colliding nuclei [26,27], etc. Over the years, several experimental studies have been performed by different groups from across the world in order to know and understand the factors influencing the onset and presence of QF in fusion-fission reactions [3,28–30] using one or more of the mentioned variables as tools.

As in QF, formation of the compact mononuclear system equilibrated in all degrees of freedom is not achieved; it hinders the fusion cross section of SHEs. At near-barrier energies, the transfer of a few nucleons from projectile to target is also a competing process [31], and sometimes could be a dominating noncompound process still leading to fission but fragments originating from such fission will have different mass angle correlations as well as angular anisotropies as compared to events originating from compound nucleus fission [32–34].

The mass asymmetric fission is well known in the spontaneous and low-energy fission of most actinide nuclei. The observed asymmetric shape of fission fragment mass

*Corresponding author: hardev79@gmail.com

TABLE I. Relevant parameters for ^{28}Si + ^{160}Gd and ^{12}C + ^{178}Hf reactions. V_b is the barrier energy in the laboratory frame, χ is the fissility, and β_2 is the quadrupole deformation.

Reaction	V_b (MeV)	$Z_P Z_T$	χ	α	α_{BG}	β_2
^{28}Si + ^{160}Gd	127	896	0.670	0.702	0.818	0.351
^{12}C + ^{178}Hf	65.5	432	0.667	0.874	0.816	0.278

distributions could be explained theoretically by taking into account the shell structure of the fragments [35,36]. However, asymmetric split in β-delayed fission of neutron-deficient ^{180}Hg is in total contrast to the expectations based on the above said argument [37,38]. This observation and subsequent experiments on fragment mass distributions from the fission of relatively neutron-deficient nuclei at low excitation energies have found the presence of QF in the form of asymmetric mass split and/or broader mass distributions [26,27,39–44]. However, a consistent picture of the QF process in general and for neutron-deficient nuclei, in particular, is far from over.

In the present study, we have measured the fragment mass distributions for ^{188}Pt and ^{190}Pt nuclei populated through ^{28}Si + ^{160}Gd and ^{12}C + ^{178}Hf reactions at energies around and above the barrier. The relevant parameters related to both the reactions are mentioned in Table I.

This systematic study of the variation of the width of fragment mass distribution provides the opportunity to explore further the nature of noncompound processes. The paper is organized as follows: The experimental details are described in Sec. II, while Sec. III describes the data analysis method. In Sec. IV, the experimental results and discussion are presented, and lastly, the summary and conclusions are given in Sec. V.

II. EXPERIMENTAL DETAILS

The experiment was carried out at the Inter-university Accelerator Centre (IUAC), New Delhi, India. Pulsed beams of ^{28}Si and ^{12}C in the laboratory energy ranges of 120–140 MeV and 60–88.2 MeV were bombarded on ^{160}Gd (≈220 μg/cm^2 on 20 μg/cm^2 carbon backing) and ^{178}Hf (≈260 μg/cm^2 on 30 μg/cm^2 carbon backing) targets, respectively. The details of targets preparation are reported in the Ref. [45,46]. Pulsed beams had a repetition rate of 250 ns and beam spread of ≈1 ns for ^{28}Si and ≈700–800 ps, in the case of ^{12}C.

The coincident fission fragments were detected using two large area (16 × 11 cm) multiwire proportional counters (MWPCs) kept at folding angle for respective reactions. Each of MWPC detectors covered the angular range of ±13° around the detector center and has a position resolution of ≈1.2 mm. Detectors were placed at the folding angles on movable arms inside the general purpose scattering chamber (GPSC), 1.5 m in diameter. The detectors were operated with isobutane gas at a pressure of about 6 mbar to make them almost transparent to elastic and quasielastic events. The time of flight (TOF) of each fragment was recorded with regard to the radio frequency (rf) timing. The target ladder was rotated with respect to the beam direction in order to avoid shadowing either of the two detectors.

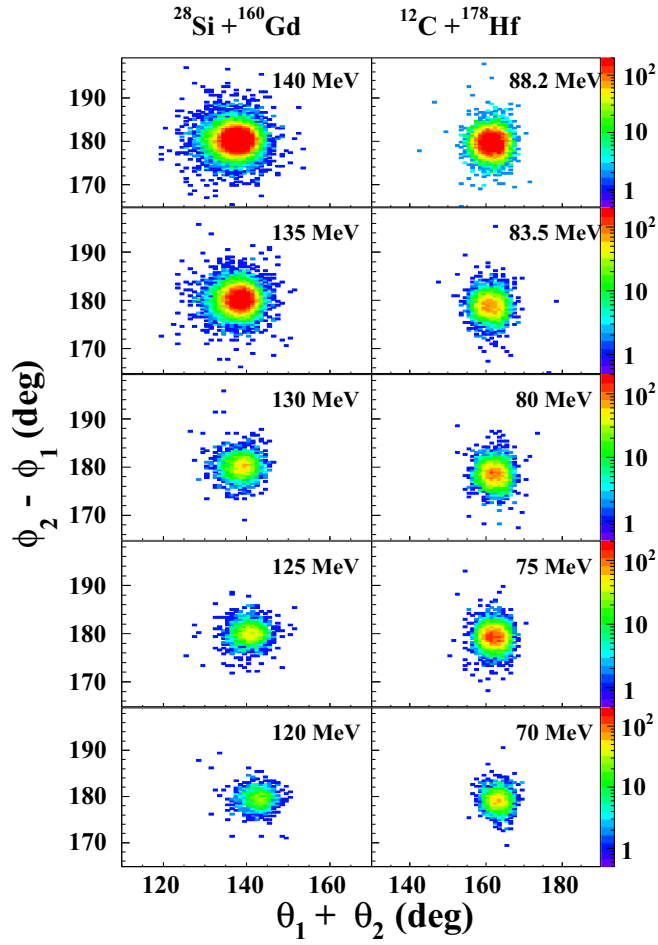

FIG. 1. Distribution of polar (θ) and azimuthal (ϕ) correlations for the ^{12}C + ^{178}Hf and ^{28}Si + ^{160}Gd reactions.

The data were collected in event mode using FREEDOM acquisition software [47]. Energy loss corrections were applied for the beam as well as for fragments in the target backing and half the target thickness using energy loss formalism of SRIM [48]. Beam monitoring was done by counting the elastically scattered beam using two silicon surface barrier detectors (SSBD) placed at ±10° with regard to the beam direction.

III. DATA ANALYSIS

The event mode data from two MWPCs consist of fission TOF and position information (X, Y). The X and Y position information was obtained from the wire grids using the delay line readout technique and TOF signals from the central wire frame of each MWPCs [49,50]. The data were analyzed using the LAMPS software [51].

The position calibration was done using the known geometry of the detectors. These X and Y calibrated positions were then converted to spherical polar coordinates θ and ϕ. The folding angle distributions were constructed for all energy points and were found to be consistent with the expected value of full momentum transfer (FMT) events. Figure 1 shows the correlation plot of polar and azimuthal angle of

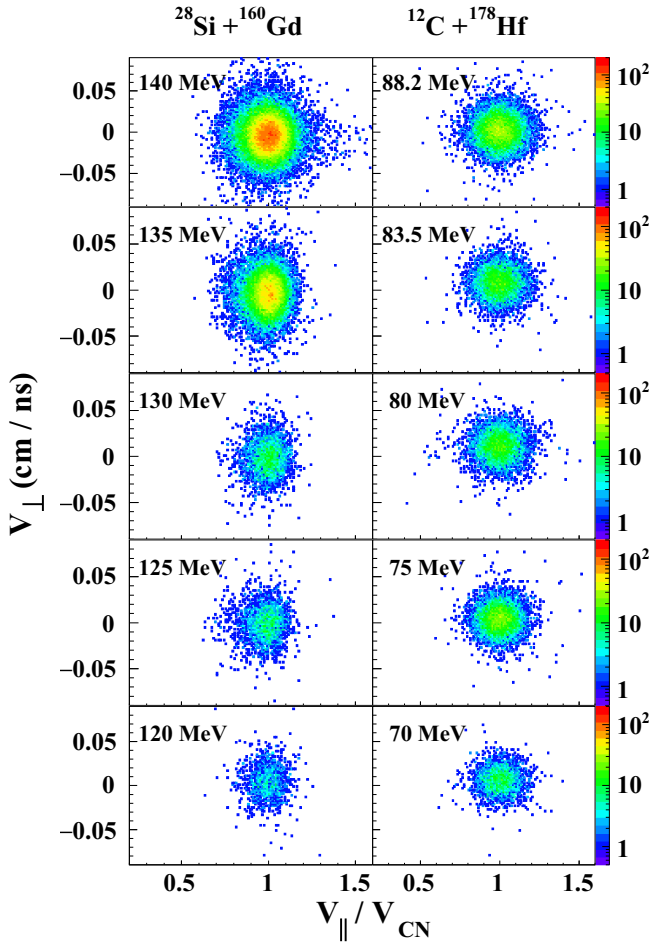

FIG. 2. Measured velocity distribution of fission fragments for both the reactions. The full momentum transfer events corresponds to the intense band around the velocity coordinates $(V_\parallel/V_{\rm cn}, V_\perp) = (1, 0)$.

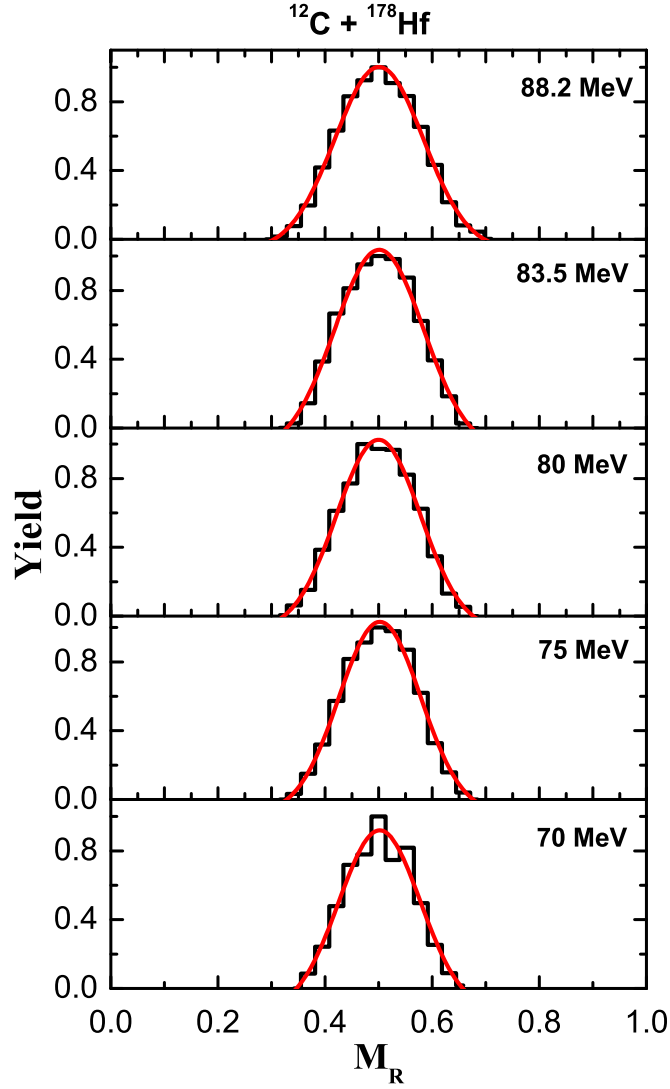

FIG. 3. The experimental mass ratio (M_R) distributions (black histogram) for the ^{12}C + ^{178}Hf reaction. Red curve represents the Gauss fit to the data.

fission fragments measured for both the reactions at different laboratory energies.

The fragments originating from fusion followed by fission were selected by imposing the condition of FMT of fissionlike events, using the correlation of the velocities of the fissioning system ($V_\parallel$) in the beam direction relative to the compound nucleus (CN) recoil velocity ($V_{\rm cn}$) and the velocity component perpendicular to the reaction plane ($V_\perp$). The expression for these components are given by [52,53]

$$V_\parallel = \frac{u_1 w_2 + u_2 w_1}{u_1 + u_2}, \tag{1}$$

$$V_\perp = \frac{u_1 u_2 \sin\phi_{12}}{\sqrt{u_1^2 + u_2^2 - 2u_1 u_2 \cos\phi_{12}}}, \tag{2}$$

where w_1, w_2 and u_1, u_2 are the measured velocity vectors decomposed into orthogonal components parallel and perpendicular to the beam axis, respectively ($w_1 = v_1\cos\theta_1$, $w_2 = v_2\cos\theta_2$, $u_1 = v_1\sin\theta_1$, $u_2 = v_2\sin\theta_2$, where v_1, v_2 and θ_1, θ_2 are the velocities and the scattering angles measured with regard to the beam direction). ϕ_{12} is the azimuthal folding angle.

The events originating from the FMT fission are shown by the intense region around the velocity coordinates $(V_\parallel/V_{\rm cn}, V_\perp) = (1, 0)$. The correlation between the measured $V_\perp$ and $V_\parallel/V_{\rm cn}$ for fission events for both the reactions is displayed in Fig. 2. The fission fragments masses were determined from TOF difference between the correlated fragments, the azimuthal and polar angles, the momenta, and the recoil velocities for each event using the following expressions [54–56]:

$$m_1 = \frac{t_1 - t_2 + \delta t_o + M_{\rm CN}\frac{d_2}{p_2}}{\frac{d_2}{p_2} + \frac{d_1}{p_1}}, \tag{3}$$

$$m_2 = M_{\rm CN} - m_1, \tag{4}$$

where t_1, t_2 are the flight times over the flight paths d_1 and d_2 of the fission fragments having masses m_1 and m_2, respectively. $M_{\rm CN}$ is the mass of compound nucleus. The momenta of fission fragments p_1 and p_2 in the laboratory frame can

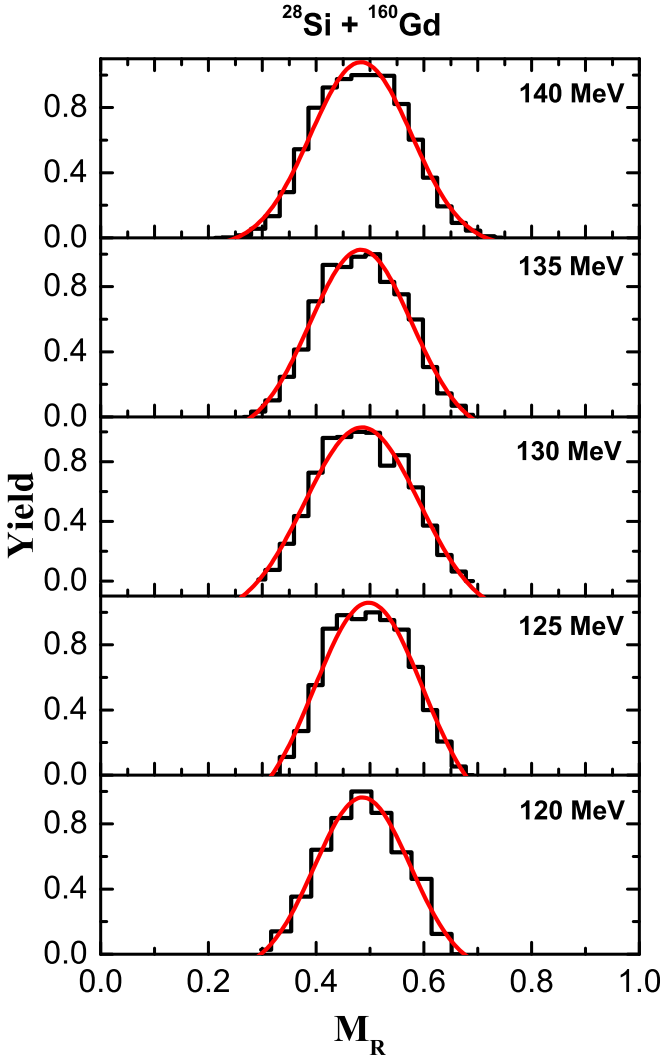

FIG. 4. The experimental mass ratio (M_R) distributions (black histogram) for ^{28}Si + ^{160}Gd reaction. Red curve represents the Gauss fit to the data.

be obtained by application of proper kinematic transformation and conservation of linear momentum.

IV. EXPERIMENTAL RESULTS AND DISCUSSION

For the reactions under consideration, using the formalism mentioned in the previous section, fission fragment mass distributions (FFMDs) were obtained for both the isotopes of Pt. The experimental mass ratio ($M_R = M_1/M_{\rm CN}$) distributions for both the reactions are shown in Figs. 3 and 4. The M_R distributions are peaked around $M_{\rm CN}/2$ and are reproducible with a single Gaussian at all studied energies. The variance of the fission fragment M_R distributions as a function of excitation energies measured for both the reactions are shown in Fig. 5.

Although the overall behavior of the width of mass distributions for both the reactions does not show any significant variation with the change in excitation energy, relatively broader mass distributions observed for the ^{28}Si + ^{160}Gd reaction at all studied energies signify the presence of events originating from noncompound processes.

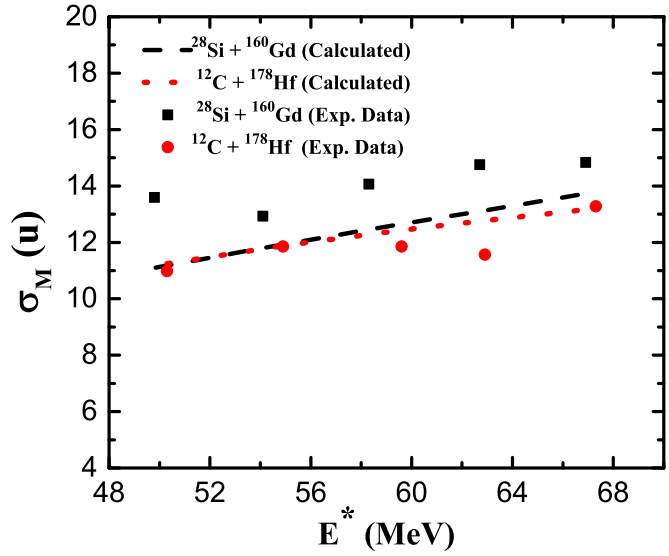

FIG. 5. Variation of the experimental fragment mass width (σ_m) values for the two reactions with excitation energy. The calculated values are shown by the dotted and dashed lines.

According to the saddle point model, the width of fission fragment mass distributions mainly depends on the excitation energy and has weaker linear dependence on the mean square angular momentum. In the case of equilibrated CN, the variance (σ_m^2) of the fragment mass distribution is linearly related to the saddle-point temperature (T) and the mean square angular momentum $\langle l^2 \rangle$ [22,57],

$$\sigma_m^2 = \lambda T + \beta \langle l^2 \rangle, \tag{5}$$

where λ (related to the stiffness of the potential energy landscape at the top of the barrier) and β are fitting constants. The saddle-point temperature T is given by [22]

$$T = \sqrt{\frac{E_{\rm c.m.} + Q - B_f - E_{\rm rot} - \nu_{\rm pre} E_n}{a}}, \tag{6}$$

where E$_{cm}$ represents the center-of-mass energy, Q is the Q value of the reaction, and B_f and $E_{\rm rot}$ are the fission barrier height and the rotational energy at average angular momentum, respectively, and are calculated using the rotating finite range model (RFRM) of Sierk [58]. The number of prefission neutrons, $\nu_{\rm pre}$, was estimated using the empirical expression given by Itkis *et al.* [59]. E_n is the average excitation energy lost due to evaporation of one neutron from the compound nucleus prior to the system reaching the saddle point. a ($a = A_{\rm CN}/10\,{\rm MeV}^{-1}$) is the nuclear level density parameter. The potential parameters (V_o, r_o, and a) for ^{28}Si + ^{160}Gd and ^{12}C + ^{178}Hf reactions are shown in Table II. The $\langle l^2 \rangle$ values used in the calculation are estimated using couple channel code CCFULL [60]. The constants, λ and β, were estimated by fitting the σ_m value for the ^{12}C + ^{178}Hf reaction, which proceeds through the formation of fully equilibrated CN. The best-fitted parameters were found to be $\lambda = 95$ and $\beta = 0.06$ and are consistent with data presented for similar nuclei [61]. The

TABLE II. The potential parameters (V_o, r_o, and a) for ^{28}Si + ^{160}Gd and ^{12}C + ^{178}Hf reactions.

System	V_o (MeV)	r_o (fm)	a (fm)
^{28}Si + ^{160}Gd	78.83	1.18	0.672
^{12}C + ^{178}Hf	58.49	1.18	0.645

same set of λ and β values should reproduce the experimental fragment mass width values for the ^{28}Si + ^{160}Gd system as well.

Figure 5 shows the experimental and calculated σ_m as a function of CN excitation energy for the two systems. The σ_m values obtained from the fitting of mass ratio plot are also tabulated in Table III, where, E^*_{saddle} is the excitation energy at the saddle. For both systems, the σ_m values shows a monotonic increase with the increase in excitation energy. It can be seen from the figure that the experimental values are in reasonable agreement with the saddle-point model calculations for the ^{12}C + ^{178}Hf reaction, whereas calculated and measured variance has a mismatch for all studied energies for the ^{28}Si + ^{160}Gd reaction. This discrepancy could either be because of the presence of events originating from QF process or it could also arise due to a possible influence of angular momentum on fission fragment mass distributions.

In order to explore the possible effects of angular momentum dependence of fragment mass distributions, in figure 6, the variation of $\langle l^2 \rangle$ of the composite system is plotted as a function of excitation energy, E^*. Around the excitation energy of 55 MeV, where the values of mean square angular momentum are same for both the reactions, the measured width of the mass distribution is still higher for ^{28}Si + ^{160}Gd reaction compared to that for ^{12}C + ^{178}Hf. Even at higher excitation energies, the increased values of $\langle l^2 \rangle$ for ^{28}Si + ^{160}Gd reaction do not have any significant effect on the calculated width of the mass distributions, as shown by the dashed line, due to the smaller value of β in Eq. (5). Clearly, the calculated width deviates from the observed higher width for the reaction ^{28}Si + ^{160}Gd in the measured energy range. Therefore, the possibility of angular momentum being a contributing factor

TABLE III. The width of the fission fragment M_R distributions and the excitation energies measured for ^{28}Si + ^{160}Gd and ^{12}C + ^{178}Hf reactions.

System	CN	E^*(MeV)	E^*_{saddle}(MeV)	σ_{MR}
		66.9	31.0	0.0789 ± 0.0036
		62.6	28.6	0.0785 ± 0.0042
^{28}Si + ^{160}Gd	^{188}Pt	58.4	26.1	0.0748 ± 0.0039
		54.1	23.5	0.0688 ± 0.0039
		49.8	21.0	0.0723 ± 0.0040
		67.3	31.7	0.0699 ± 0.0038
		62.9	28.9	0.0609 ± 0.0035
^{12}C + ^{178}Hf	^{190}Pt	59.7	26.8	0.0624 ± 0.0037
		55.0	24.0	0.0628 ± 0.0038
		50.3	21.0	0.0578 ± 0.0038

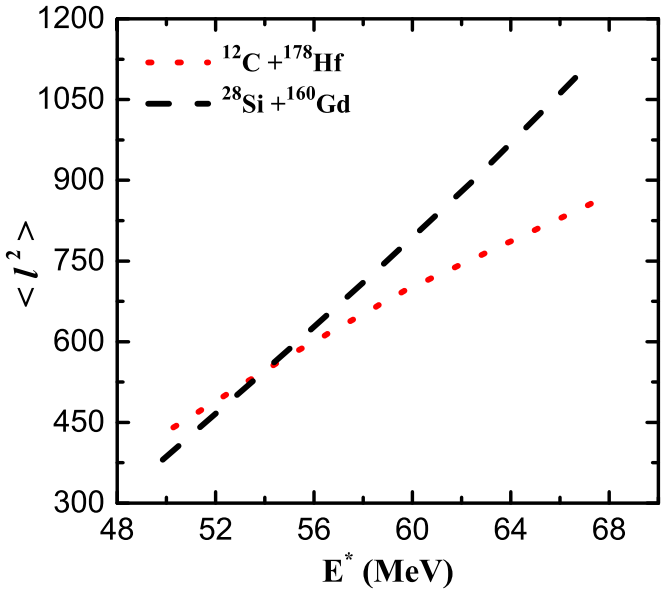

FIG. 6. Variation of mean square angular momentum with excitation energy for the two reactions.

to the observed anomaly in mass distributions between the two reactions can be ruled out. The presence of nonequilibrium processes in the fission of ^{188}Pt, populated via ^{28}Si + ^{160}Gd reaction, in the studied energy domain, could be due to the fact that it is being relatively more neutron deficient than ^{190}Pt. However, earlier studies has established that the CN formation mechanism could be different based on the value of entrance channel mass asymmetry α with regard to α_{BG}, as the fusion paths followed by the reaction with $\alpha > \alpha_{BG}$ and $\alpha < \alpha_{BG}$ are quite different, even though both the systems form similar CNs [62]. For the reaction ^{12}C + ^{178}Hf with entrance channel mass asymmetry α (0.874) higher than α_{BG} (0.816), the mass flow is from the projectile to the target, thereby leading to a compact mononucleus. On the other hand, for the reaction ^{28}Si + ^{160}Gd, with an entrance channel mass asymmetry (0.702) less than the α_{BG}, the mass flow is in the direction of a more symmetric dinuclear system and this could well lead to different widths of the mass distributions as observed in the present study. The present study confirms the existence of the nonequilibrated/QF processes in the studied energy domain for the fission of ^{188}Pt, a neutron-deficient isotope of Pt, even though mass distributions do not show any pronounced asymmetric or three-peak behavior. It would be of interest to measure the mass distributions for such reactions going further below the barrier.

V. SUMMARY AND CONCLUSIONS

In the present work, we have measured the mass distributions of isotopes of Pt (^{188,190}Pt), populated through the fusion reactions ^{28}Si + ^{160}Gd and ^{12}C + ^{178}Hf, respectively, at energies around and above the Coulomb barrier. The systematic trends of the mass widths were investigated as a function of excitation energy of the CN. It is observed that the width of mass distributions for the fission of ^{188}Pt are relatively broader

than the one calculated on the basis of the saddle-point model, indicating a contribution from QF. Our measurements could be an indication that with even a small reduction in neutron number in Pt isotopes (^{190}Pt to ^{188}Pt), there is a transition of reaction mechanism from fusion-fission to QF. On the other hand, entrance channel dynamics could also play a role in deciding the fate of the excited CN. It will be interesting to have experimental data going further below the barrier to see if the observed behavior changes to completely asymmetric fission, as observed in some other neutron-deficient systems. Further, exploring the potential energy surface (PES) for the two systems performing the dynamical model calculations could help in better understanding the fission dynamics in such reactions.

ACKNOWLEDGMENTS

The authors are thankful to IUAC, New Delhi, India, for all the necessary support during the experiment. One of the authors (Kavita) acknowledges IUAC, New Delhi, and UGC-BSR, New Delhi, for the financial support for carrying out the research work. We are thankful to Professor W. U. Schröder and Dr. S. Bhattacharya for the feedback on manuscript.

[1] Y. T. Oganessian, V. K. Utyonkov, Y. V. Lobanov, F. S. Abdullin, A. N. Polyakov, R. N. Sagaidak, I. V. Shirokovsky, Y. S. Tsyganov, A. A. Voinov, G. G. Gulbekian *et al.*, Phys. Rev. C **74**, 044602 (2006).
[2] S. Hofmann and G. Münzenberg, Rev. Mod. Phys. **72**, 733 (2000).
[3] B. B. Back, Phys. Rev. C **31**, 2104 (1985).
[4] D. J. Hinde, R. du Rietz, M. Dasgupta, R. G. Thomas, and L. R. Gasques, Phys. Rev. Lett. **101**, 092701 (2008).
[5] K. Nishio, S. Mitsuoka, I. Nishinaka, H. Makii, Y. Wakabayashi, H. Ikezoe, K. Hirose, T. Ohtsuki, Y. Aritomo, and S. Hofmann, Phys. Rev. C **86**, 034608 (2012).
[6] D. J. Hinde, D. Y. Jeung, E. Prasad, A. Wakhle, M. Dasgupta, M. Evers, D. H. Luong, R. du Rietz, C. Simenel, E. C. Simpson *et al.*, Phys. Rev. C **97**, 024616 (2018).
[7] E. Prasad, D. J. Hinde, E. Williams, M. Dasgupta, I. P. Carter, K. J. Cook, D. Y. Jeung, D. H. Luong, C. S. Palshetkar, D. C. Rafferty *et al.*, Phys. Rev. C **96**, 034608 (2017).
[8] T. K. Ghosh, K. Banerjee, C. Bhattacharya, S. Bhattacharya, S. Kundu, P. Mali, J. K. Meena, G. Mukherjee, S. Mukhopadhyay, and T. K. Rana, Phys. Rev. C **79**, 054607 (2009).
[9] E. M. Kozulin, G. N. Knyazheva, K. V. Novikov, I. M. Itkis, M. G. Itkis, S. N. Dmitriev, Y. T. Oganessian, A. A. Bogachev, N. I. Kozulina, I. Harca *et al.*, Phys. Rev. C **94**, 054613 (2016).
[10] M. G. Itkis, E. Vardaci, I. M. Itkis, G. N. Knyazheva, and E. M. Kozulin, Nucl. Phys. A **944**, 204 (2015).
[11] J. Tõke, R. Bock, G. X. Dai, A. Gobbi, S. Gralla, K. D. Hildenbrand, J. Kuzminski, W. F. J. Müller, A. Olmi, H. Stelzer *et al.*, Nucl. Phys. A **440**, 327 (1985).
[12] J. P. Blocki, H. Feldmeier, and W. J. Swiatecki, Nucl. Phys. A **459**, 145 (1986).
[13] M. G. Itkis, A. A. Bogachev, I. M. Itkis, J. Kliman, G. N. Knyazheva, N. A. Kondratiev, E. M. Kozulin, L. Krupa, Y. T. Oganessian, I. V. Pokrovsky *et al.*, Nucl. Phys. A **787**, 150c (2007).
[14] R. Rafiei, R. G. Thomas, D. J. Hinde, M. Dasgupta, C. R. Morton, L. R. Gasques, M. L. Brown, and M. D. Rodriguez, Phys. Rev. C **77**, 024606 (2008).
[15] W. J. Swiatecki, Phys. Scr. **24**, 113 (1981).
[16] R. G. Thomas, R. K. Choudhury, A. K. Mohanty, A. Saxena, and S. S. Kapoor, Phys. Rev. C **67**, 041601(R) (2003).
[17] A. C. Berriman, D. J. Hinde, M. Dasgupta, C. R. Morton, R. D. Butt and J. O. Newton, Nature (London) **413**, 144 (2001).
[18] C. Yadav, R. G. Thomas, R. K. Choudhury, P. Sugathan, A. Jhingan, S. Appannababu, K. S. Golda, D. Singh, I. Mukul, J. Gehlot *et al.*, Phys. Rev. C **86**, 034606 (2012).
[19] E. Williams, D. J. Hinde, M. Dasgupta, R. du Rietz, I. P. Carter, M. Evers, D. H. Luong, S. D. McNeil, D. C. Rafferty, K. Ramachandran *et al.*, Phys. Rev. C **88**, 034611 (2013).
[20] A. Chaudhuri, A. Sen, T. K. Ghosh, K. Banerjee, J. Sadhukhan, S. Bhattacharya, P. Roy, T. Roy, C. Bhattacharya, Md. A. Asgar *et al.*, Phys. Rev. C **94**, 024617 (2016).
[21] M. Abe, KEK Preprint 86-26, KEK TH-128, 1986.
[22] G. N. Knyazheva, E. M. Kozulin, R. N. Sagaidak, A. Y. Chizhov, M. G. Itkis, N. A. Kondratiev, V. M. Voskressensky, A. M. Stefanini, B. R. Behera, L. Corradi *et al.*, Phys. Rev. C **75**, 064602 (2007).
[23] K. Banerjee, T. K. Ghosh, S. Bhattacharya, C. Bhattacharya, S. Kundu, T. K. Rana, G. Mukherjee, J. K. Meena, J. Sadhukhan, S. Pal *et al.*, Phys. Rev. C **83**, 024605 (2011).
[24] T. K. Ghosh, S. Pal, K. S. Golda, and P. Bhattacharya, Phys. Lett. B **627**, 26 (2005).
[25] R. K. Choudhury and R. G. Thomas, J. Phys.: Conf. Ser. **282**, 012004 (2011).
[26] E. Prasad, D. J. Hinde, K. Ramachandran, E. Williams, M. Dasgupta, I. P. Carter, K. J. Cook, D. Y. Jeung, D. H. Luong, S. McNeil *et al.*, Phys. Rev. C **91**, 064605 (2015).
[27] K. Nishio, A. N. Andreyev, R. Chapman, X. Derkx, C. E. Düllmann, L. Ghys, F.P. Heβberger, K. Hirose, H. Ikezoe, J. Khuyagbaatar *et al.*, Phys. Lett. B **748**, 89 (2015).
[28] E. Prasad, K. M. Varier, R. G. Thomas, P. Sugathan, A. Jhingan, N. Madhavan, B. R. S. Babu, R. Sandal, S. Kalkal, S. Appannababu *et al.*, Phys. Rev. C **81**, 054608 (2010).
[29] C. J. Lin, R. du Rietz, D. J. Hinde, M. Dasgupta, R. G. Thomas, M. L. Brown, M. Evers, L. R. Gasques, and M. D. Rodriguez, Phys. Rev. C **85**, 014611 (2012).
[30] K. Nishio, H. Ikezoe, I. Nishinaka, S. Mitsuoka, K. Hirose, T. Ohtsuki, Y. Watanabe, Y. Aritomo, and S. Hofmann, Phys. Rev. C **82**, 044604 (2010).
[31] P. Bhattacharya, N. Majumdar, P. Basu, M. L. Chatterjee, D. C. Biswas, A Saxena, V. S. Ambedkar, R. K. Choudhury and D. M. Nadkarni, Nuovo Cim. A **108**, 819 (1995).
[32] K. Hirose, K. Nishio, S. Tanaka, R. Leguillon, H. Makii, I. Nishinaka, R. Orlandi, K. Tsukada, J. Smallcombe, M. J. Vermeulen *et al.*, Phys. Rev. Lett. **119**, 222501 (2017).
[33] K. Nishio, K. Hirose, M. Vermeulen, H. Makii, R. Orlandi, K. Tsukada, M. Asai, A. Toyoshima, T. K. Sato, Y. Nagame *et al.*, EPJ Web Conf. **169**, 00013 (2018).
[34] A. Pal, S. Santra, D. Chattopadhyay, A. Kundu, A. Jhingan, P. Sugathan, N. Saneesh, M. Kumar, N. L. Singh, A. Yadav *et al.*, Phys. Rev. C **98**, 031601(R) (2018).

[35] P. Möller, D. G. Madland, A. J. Sierk, and A. Iwamoto, Nature (London) **409**, 785 (2001).
[36] Y. Oganessian, J. Phys. G: Nucl. Part. Phys. **34**, R165 (2007).
[37] A. N. Andreyev, J. Elseviers, M. Huyse, P. Van Duppen, S. Antalic, A. Barzakh, N. Bree, T. E. Cocolios, V. F. Comas, J. Diriken *et al.*, Phys. Rev. Lett. **105**, 252502 (2010).
[38] J. Elseviers, A. N. Andreyev, M. Huyse, P. Van Duppen, S. Antalic, A. Barzakh, N. Bree, T. E. Cocolios, V. F. Comas, J. Diriken *et al.*, Phys. Rev. C **88**, 044321 (2013).
[39] A. V. Andreev, G. G. Adamian, and N. V. Antonenko, Phys. Rev. C **93**, 034620 (2016).
[40] A. N. Andreyev, S. Antalic, D. Ackermann, L. Bianco, S. Franchoo, S. Heinz, F. P. Heβberger, S. Hofmann, M. Huyse, Z. Kalaninová *et al.*, Phys. Rev. C **87**, 014317 (2013).
[41] P. Möller, J. Randrup, and A. J. Sierk, Phys. Rev. C **85**, 024306 (2012).
[42] L. Ghys, A. N. Andreyev, M. Huyse, P. Van Duppen, S. Sels, B. Andel, S. Antalic, A. Barzakh, L. Capponi, T. E. Cocolios *et al.*, Phys. Rev. C **90**, 041301(R) (2014).
[43] M. Warda, A. Staszczak, and W. Nazarewicz, Phys. Rev. C **86**, 024601 (2012).
[44] I. Tsekhanovich, A. N. Andreyev, K. Nishio, Denis-Petit, K. Hirose, H. Makii, Z. Matheson, K. Morimoto, K. Morita, W. Nazarewicz *et al.*, Phys. Lett. B **790**, 583 (2019).
[45] Kavita, S. R. Abhilash, D. Kabiraj, K. S. Golda, S. Chopra, S. Ojha, G. R. Umapathy, D. Mehta, G. Singh, S. Kumar *et al.*, Vacuum **145**, 11 (2017).
[46] Kavita, S. R. Abhilash, K. S. Golda, D. Kabiraj, R. Kumar, R. Dubey, N. Kumar, and H. Singh, DAE Symp. Nucl. Phys. **62**, 1102 (2017).
[47] B. P. A. Kumar, E. T. Subramaniam, K. Singh, and R. K. Bhowmik, *FREEDOM high-speed DAS* (SANAI, Trombay, India, 1997).
[48] J. F. Ziegler, *SRIM2000 (TRIM) Stopping and Ranges of Ions in Matter, ver. 2000* (IBM Research, Yorktown, NY, 2000).
[49] A. Jhingan, P. Sugathan, K. S. Golda, R. P. Singh, T. Varughese, H. Singh, B. R. Behera, and S. K. Mandal, Rev. Sci. Instrum. **80**, 123502 (2009).
[50] A. Jhingan, G. Kaur, N. Saneesh, R. Mahajan, M. Thakur, T. Banerjee, R. Dubey, P. Sharma, A. Yadav, R. Ahuja *et al.*, DAE Symp. Nucl. Phys. **60**, 936 (2015).
[51] http://www.tifr.res.in/~pell//lamps_files/vme.html.
[52] D. J. Hinde, M. Dasgupta, J. R. Leigh, J. C. Mein, C. R. Morton, J. O. Newton, and H. Timmers, Phys. Rev. C **53**, 1290 (1996).
[53] I. Mukul, S. Nath, K. S. Golda, A. Jhingan, J. Gehlot, E. Prasad, S. Kalkal, M. B. Naik, T. Banerjee, T. Varughese *et al.*, Phys. Rev. C **92**, 054606 (2015).
[54] T. K. Ghosh, S. Pal, T. Sinha, S. Chattopadhyay, K. S. Golda, and P. Bhattacharya, Nucl. Inst. Methods Phys. Res. A **540**, 285 (2005).
[55] R. G. Thomas, D. J. Hinde, D. Duniec, F. Zenke, M. Dasgupta, M. L. Brown, M. Evers, L. R. Gasques, M. D. Rodriguez, and A. Diaz-Torres, Phys. Rev. C **77**, 034610 (2008).
[56] R. K. Choudhury, A. Saxena, A. Chatterjee, D. V. Shetty, S. S. Kapoor, M. Cinausero, L. Corradi, E. Farnea, E. Fioretto, A. Gadea *et al.*, Phys. Rev. C **60**, 054609 (1999).
[57] B. B. Back, P. B. Fernandez, B. G. Glagola, D. Henderson, S. Kaufman, J. G. Keller, S. J. Sanders, F. Videbæk, T. F. Wang and B. D. Wilkins, Phys. Rev. C **53**, 1734 (1996).
[58] A. J. Sierk, Phys. Rev. C **33**, 2039 (1986).
[59] M. G. Itkis and A. Y. Rusanov, Phys. Part. Nucl. **29**, 160 (1998).
[60] K. Hagino, N. Rowley, and A. T. Kruppa, Comput. Phys. Commun. **123**, 143 (1999).
[61] M. G. Itkis and A. Ya. Rusanov, Yad. Fiz. **52**, 23 (1990).
[62] H. Singh, K. S. Golda, S. Pal, Ranjeet, R. Sandal, B. R. Behera, G. Singh, A. Jhingan, R. P. Singh, P. Sugathan *et al.*, Phys. Rev. C **78**, 024609 (2008).